Sampling frequency fluctuations of the Sensors & Software SPIDAR Ground Penetrating Radar: impact on probing passive surface acoustic wave delay lines for pollution sensing

D. Rabus, L. Arapan, T. Pierre, J.-M Friedt, F. Chérioux

Index Terms—**GPR, SAW, sensor, stability, delay line**

***Abstract*—In the context of the subsurface pollutant detection using cooperative targets probed by Ground Penetrating RADAR (GPR), we assess the sampling frequency stability of the instrument as needed to make sure any time delay variation between echoes is associated with sub-surface chemical detection and not with instrument drift. Thanks to surface acoustic wave transducers designed as GPR cooperative targets, the sampling frequency of the Sensors and Software SPIDAR GPR control unit is characterized for short and long term sampling rate stabilities. The long term stability of the instrument is below the phase measurement noise of the surface acoustic wave cooperative target. However, short term (within each trace) phase fluctuations are observed, hinting at short term stroboscopic delay synthesis artifacts. Having demonstrated the stability of the baseline, we demonstrate gas-phase pollutant detection in the sub-surface environment using GPR interrogation of a surface acoustic wave sensor functionalized with a dedicated coating for reacting with hydrogen sulfide. Finally, for on-site long term monitoring, an embedded vector network analyzer is shown to exhibit sufficient stability and the targeted performance for this measurement by recovering the time-domain response through the inverse Fourier transform of the frequency swept characterization of the sensor.**

I. Introduction

Surface acoustic wave (SAW) transducers [1], [2], [3], using the conversion of an electromagnetic wave to an acoustic wave confined to the surface of a piezoelectric substrate, have been demonstrated to be reliable cooperative targets for complementing Ground Penetrating RADAR (GPR) sub-surface measurements with tagging and sensing capability [4]. Sub-surface measurement is ideally fitted to passive, wireless cooperative targets since battery lifetime is expected to be shorter than the usage duration of the facility the sensor is fitted to (pipeline and industrial infrastructure, underground utilities such as water pipes or electricity transport cables), while wires connecting the sensor to the surface will be prone to aging and disturbance during shallow soil handling (e.g. construction work). Indeed, urbanized areas claim up to 47 km of sub-surface utilities for every kilometer of road [5], [6], with the need for tagging and sensing such infrastructures to focus maintenance in case of failure to the appropriate area.

The authors are affiliated with the FEMTO-ST Institute, Besançon, France. Corresponding author: J.-M Friedt (e-mail: jmfriedt@femto-st.fr).

Probing chemical compound concentrations, as needed for example for pollutant sensing, is achieved by propagating an acoustic wave on the SAW sensor substrate surface after functionalization by a dedicated sensing compound. Typical acoustic velocities are 10^5 slower than the speed of light so that the 3 m long 100 MHz electromagnetic wavelength shrinks to 30 μm acoustic wave and the typical sensing film thickness is in the micrometer range, well suited for cleanroom processing technology.

GPR cooperative targets are designed by patterning interdigitated transducer (IDT) electrodes on a piezoelectric substrate – typically strongly coupled substrates such as lithium niobate YXl/128° or lithium tantalate YXl/36° – to convert the electromagnetic wave to an acoustic wave confined to the surface of the substrate. Bragg mirrors are patterned as electrodes at fixed distances to generate echoes delayed by a few hundred nanoseconds to microseconds when using millimeter-long acoustic paths (Fig. 1). These echoes are converted back to electromagnetic wave and recorded by the GPR receiver.

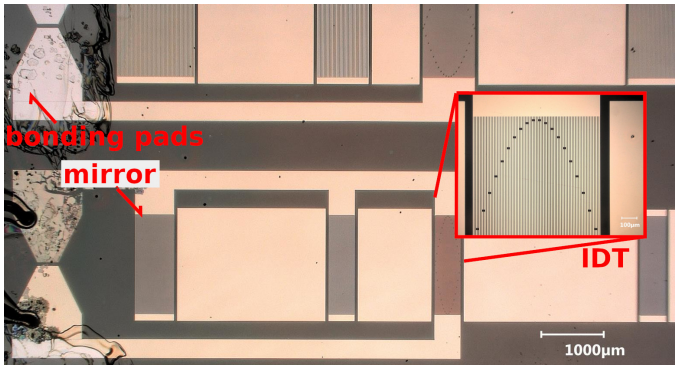

Fig. 1. Two SAW delay lines centered on 100 MHz (top) and 200 MHz (bottom) with three mirrors, two to left of the interdigitated transducer (IDT) and one to the right. Inset: zoom on the apodized IDT. The chip is coated with the sensing polymer except for the bonding pads on the left.

Mass loading, or stiffening [7], of this sensing layer will affect the boundary condition of the propagating wave, and since the acoustic velocity in an isotropic (sensing layer) medium is given by the square root of the Young modulus to the density ratio, so will the SAW acoustic velocity be impacted. Considering the distance between IDT wave and the mirrors fixed, varying the acoustic velocity is observed as a time of flight variation and measured by the GPR as echoes returned by the SAW sensor. Three frequency ranges

are considered: 100±10 MHz and 200±20 MHz as classically used in GPR investigations when depths of a few tens of centimeters to a few meters are considered, and 490±40 MHz for shallower depths but compatible with passive RADAR sub-surface measurements using non-cooperative emitters as demonstrated in [8].

Fine acoustic velocity measurement, practically identified through a phase variation, requires an accurate knowledge of the sampling frequency f_s. Indeed the sampling time at index k is converted to time t through $t = k/f_s$ and the time delay dt introduced by the sensing principle is detected as a phase variation $d\varphi$ when probing the sensor at center frequency f as $d\varphi = 2\pi dt \cdot f = 2\pi k/f_s \cdot f$ with f defined by the physical layout of the SAW transducer and f_s dependent on the recording hardware. Velocity is always measured as a delay (phase) *difference* between two echoes generated by mirrors patterned on the piezoelectric substrate in order to cancel the common delay of the emitter to sensor time of flight (Fig. 2), dependent on the emitter distance to the sensor and the permittivity of soil.

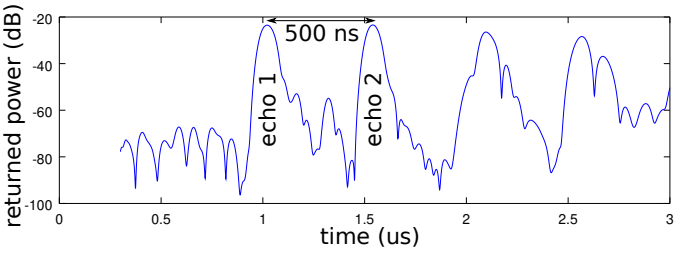

Fig. 2. Time domain characteristics of a 200 MHz SAW device designed as GPR cooperative target: the time difference of the first two echoes, allowing for fine measurement of the acoustic velocity, are analyzed throughout this document.

We had identified in the past [9] that Malå ProEx GPR hardware exhibits insufficient long term sampling rate stability due to a temperature sensitive capacitor driving the ramp generator needed for stroboscopic signal generation. Having shifted to a Sensors & Software pulseEkko GPR driven by a SPIDAR control unit for probing our sensors, we again discover varying sampling rate. While in this investigation the long term stability allows for fine detection of acoustic velocity measurement, as shown in section II, and hence chemical compound detection, we observe that the sampling rate varies within each collected trace in a reproducible way independent on the starting time or the programmed sampling rate, as will be presented in section III. Since the mean value of the phase remains the same, such issues do not prevent chemical sensor probing but might be a hindrance for users of the GPR requiring fine phase analysis such as synthetic aperture RADAR analysis (i.e. migration) as demonstrated in section V. This presentation is concluded with an alternative to stroboscopic pulsed GPR, namely embedded portable network analyzer providing a credible alternative for long term, in situ sensor monitoring (section VI).

Throughout this document, except for section V where the sensor surface is exposed to a gas being detected through its interaction with the sensing polymer, the SAW transducer is kept under stable conditions and the echoes are returned with constant delay by the cooperative target. Any fluctuation in the measured echo delay is hence attributed to the instrument probing the SAW sensor response.

II. Long term stability assessment

An initial assessment of the long term stability of the SPIDAR control unit was conducted by illuminating a 100 MHz SAW reflective delay line with the GPR and collecting samples every 500 ps (2 GHz equivalent sampling frequency, or 20 samples/period of the SAW signal) with 5200 sample long traces (2.6 μs long traces) including both echoes returned by the acoustic transducer.

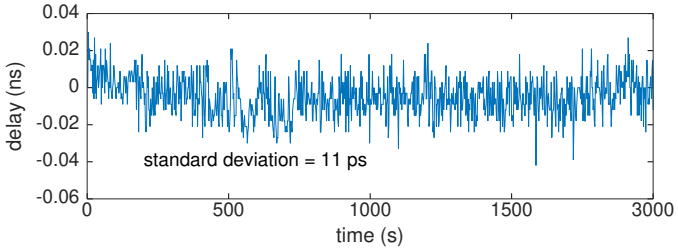

Fig. 3. Long term (40 min. long) stability measurement of a SAW delay line probed by a SPIDAR control unit, exhibiting a standard deviation on the echo delay difference (500 ns) of 11 ps.

Correlating the 400 samples including the first echo with the 400 samples including the second echo (i.e. 200 ns long windows), the position of the cross-correlation maximum is tracked. The time delay between echoes is displayed by multiplying the cross correlation maximum index by the sampling period, here 0.5 ns, as displayed in Fig. 3. The standard deviation on this measurement is 11 ps, consistent with measurements reported in [10] (5 ps jitter in static and noisy environments) on a different brand of GPR (IDS) operating at a different frequency (900 MHz) but which can be assumed to be based on similar sampling technology. For a 100 MHz delay line for which a 2π phase rotation matches a 10 ns period, a 11 ps standard deviation is equivalent to a phase standard deviation of 7 mrad or 0.4°. We will see that a typical measurement will yield phase shifts of several degrees, so that the long term stability is well below the targeted measurement variation. The SPIDAR control unit hence seems well suited to the task of measuring sub-surface sensors.

However, cross correlation provides a mean value of the phase over the integration window, here 200 ns long. An alternative approach to compute fine time delays between echoes is through the phase of the Hilbert transform of the collected traces [11].

III. Time resolved phase measurement

Hilbert transform will provide a time resolved estimate of the magnitude and phase by computing the imaginary part missing from the real signal acquisition to create an analytical signal. The phase difference of the Hilbert transform at time delays in which acoustic delay line echoes are collected is displayed in Fig. 4.

The phase fluctuation within each trace cannot be attributed to the acoustic delay line whose linear response is independent on response delay. We attribute these short term reproducible phase fluctuations to varying sampling rate within each trace.

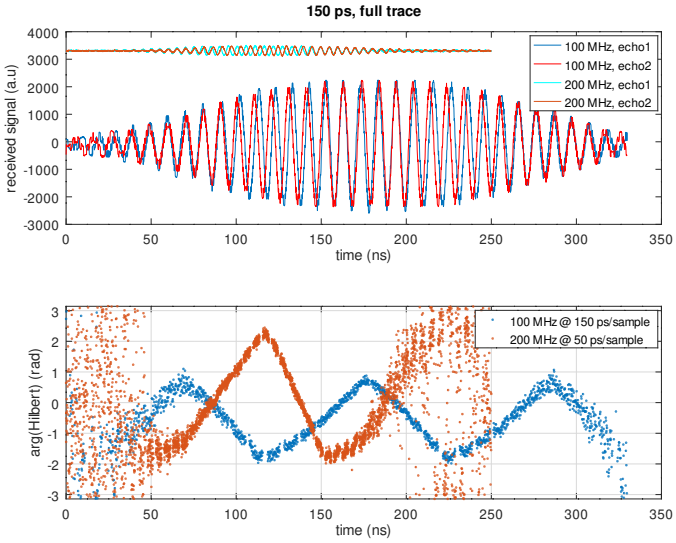

Fig. 4. Top: time domain of the first (blue) and second (red) echoes shifted in time to overlap, exhibiting the sampling time shift during the acquisition. Bottom: phase difference of the Hilbert transform of the first echo with respect to the second echo. The phase fluctuations along the trace is attributed to varying sampling rate.

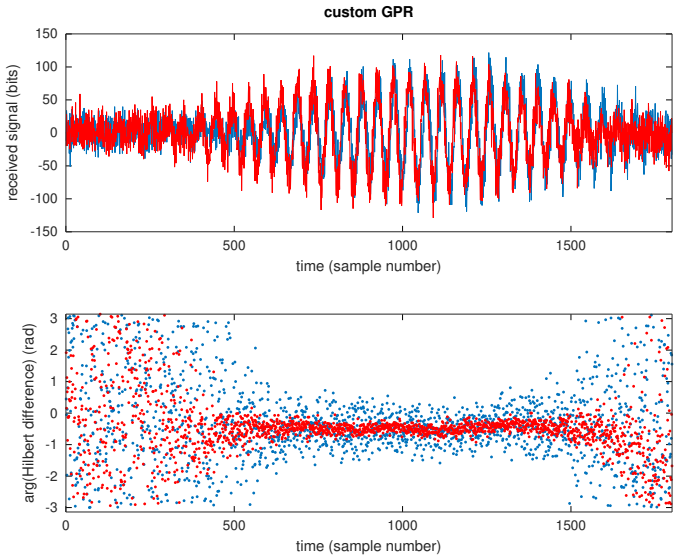

Fig. 5. SAW reflective delay line interrogation using a custom high stability GPR setup. Top the raw measurements by the receiver exhibiting the echoes returned by the SAW cooperative target, with a non-null mean value. Bottom: phase between the first and second echo within a same trace *after removing the mean value* of each trace (blue) and the application to a mean (stack) of 10 successive A-scans (red) to exhibit similar signal to noise ratio than Fig. 4. Notice that in this case the phase hardly fluctuates, indicating a constant sampling rate, here controlled by a quartz oscillator. Comparing with the result displayed on Fig. 4 emphasizes how the phase fluctuations within each acquisition has been cancelled by the custom sampling system setup as described in [12].

In order to make sure the cooperative target is not the cause of the fluctuations, the same measurement was completed with a Malå ProEx GPR and reported in [9], and a custom high stability GPR setup clocked by a quartz reference driving a high resolution counter [12]: in both cases, correlating the two echo responses within each trace exhibits a stable phase and none of the fluctuations observed with the Sensors & Software instrument (Fig. 5).

Both 100 MHz and 200 MHz acoustic reflective delay lines have been illuminated by the pulseEkko GPR fitted with the associated unshielded dipole antennas. As expected from a varying sampling period introduced by the GPR, doubling the sensor frequency doubles the phase shift observed. Considering that one period (2π radians) is 5 or 10 ns for 200 or 100 MHz respectively, ± 2 to ± 1 rad phase variations respectively are both consistent with ± 1.5 ns since $2\times 5/(2\pi) = 1\times 10/(2\pi) \simeq 1.5$ ns. Such a delay is interpreted as up to 30 sample offsets when sampling with 150 ps or 50 ps sampling intervals as selected when measuring the 100 and 200 MHz delay line respectively. This analysis will be confirmed by analyzing the GPR trigger signals, independently of acoustic transducer responses.

IV. Timebase Oscilloscope Characterization

The Hilbert transform analysis is confirmed by monitoring the trigger signal from the SPIDAR control unit to the receiver. A LeCroy 80 GS/s LabMaster 10-36Zi-A oscilloscope is used for such a measurement.

Considering the finite memory depth of 128 million samples (2 channels, for a total of 256 Msamples) of the oscilloscope, its sampling rate is reduced to 10 GS/s, allowing for a 11 ms oscilloscope trace duration matching the collection of 1100 samples by the GPR at a pulse repetition rate of 10 μs.

In this measurement, a GPR sampling interval of 500 ps was selected so that these 1100 samples last 550 ns, covering both echoes returned by the SAW transducer.

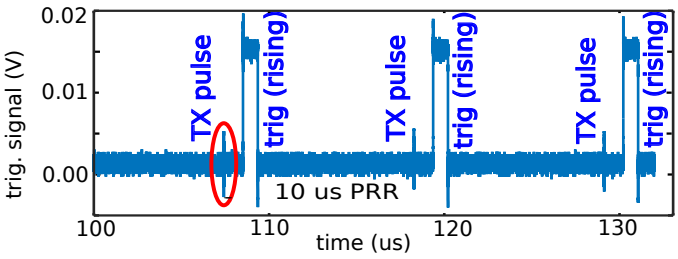

Fig. 6. Oscilloscope trace exhibiting the sampling trigger pulse and the pulse transmitted by the emitter (highlighted with the red circle for its first occurence) and coupled through the coaxial cable acting as an antenna.

A radiofrequency-grade coaxial cable is soldered between the pulseEkko receiver test point TP3 and ground TP4. TP3 is the signal received from the SPIDAR control unit, buffered by Maxim MAX961 fast comparators to prevent impact of the measurement system on the signal timing. The cable connecting the RADAR receiver to the oscilloscope acts as an antenna and picks up the transmitted signal radiated by the emitter antenna. A zoom on such a measurement on a few stroboscopic periods is exhibited in Fig. 6.

Measuring the time interval between the rising edge of the receiver acquisition trigger signal and the transmitted pulse yields Fig. 7 (bottom). This time interval is compared with the phase difference from two acoustic wave echoes collected at the same time by the GPR. Notice that the middle trace of Fig. 7 (echo phase) and bottom trace (time interval between acquisition and transmitted pulse) are not on the same time scale: both datasets indicate a varying sampling interval with a period of 200 ns (green lines as guide for the eye).

The cause of this varying sampling interval has not been investigated further due to the compact assembly of the

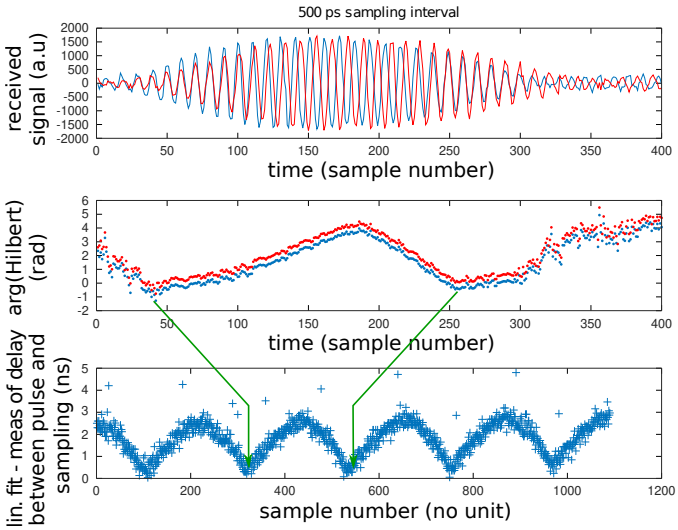

Fig. 7. Top: signal measured by the receiver including the echoes returned by the SAW cooperative target. Middle: phase between the first and second echo measured in the same trace. Bottom: time interval between the acquisition trigger rising edge and the radiofrequency pulse transmitted by the emitting antenna and picked up by the cable connecting the receiver to the oscilloscope. A linear fit ("lin. fit" on the Y-axis label) of this time interval has been subtracted to only display the variation around this linear trend. The green lines guide the eye to emphasize the same periodicity of the fluctuating sampling rate despite the different time scales of the two charts.

SPIDAR control unit. While this varying sampling rate hardly impacts SAW sensor measurements which integrate the phase over more than the 200 ns period over which the sampling rate varies, users of the GPR focusing on shorter echo delays should be cautious of such artifacts. Furthermore, it was assessed that the SPIDAR control unit temperature, in the -20 °C to $+20$ °C range, does not affect the differential measurement accuracy of the sensor echo delay difference (see Supplementary Material).

V. Subsurface sensor measurement

Having assessed the long term stability of the pulseEkko GPR controlled by a SPIDAR unit, custom software has been used to collect traces and cross-correlate both echoes to recover the fine time delay.

As a demonstration of the need for long term stability of the baseline and the ability to probe a sub-surface sensor wirelessly by illuminating a buried SAW reflective delay line with a GPR pulse and collect the echoes, a hydrogen sulfide detection is demonstrated [13]. A 200 MHz reflective delay line is functionalized with a polymer loaded with lead ions known to selectively react with the sulfur atom of hydrogen sulfide. This reaction is the classical measurement mechanism of lead-acetate soaked paper darkening upon exposure to hydrogen sulfide.

The experiment is conducted by inserting a sensor in a 3 cm-diameter PVC tube buried 30 cm deep in a sandbox. The delay between the echoes returned by the sensor is measured for 10 minutes to assess the baseline (Fig. 8). Hydrogen sulfide is produced and injected in the tube at time 700 s as the GPR keeps on collecting traces. Since hydrogen sulfide reacts with lead to create lead sulfide nanoparticles loading the polymer, the decreased acoustic velocity is observed as a phase decrease. During this dataset processing, "phase" refers to the phase of the inverse Fourier transform of the product of the Fourier transforms of the datasets including one echo and the complex conjugate for the second echo. This operation matches the cross-correlation computation through the convolution theorem in which time is reverted in one of the two terms of the product by using the complex conjugate of the Fourier transform. Such a phase matches the measurement classically performed using a network analyzer when qualifying radiofrequency devices.

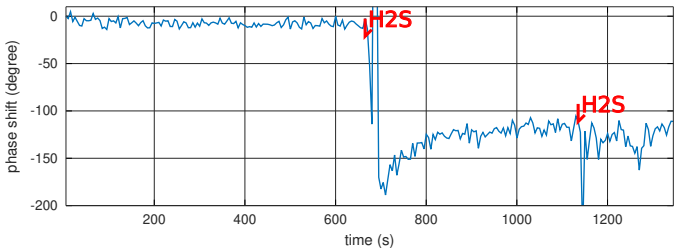

Fig. 8. Hydrogen sulfide (H_2S) detection by a functionalized SAW reflective delay line buried 30 cm deep in a sandbox. Hydrogen sulfide is produced and flown through the buried tube in which the sensor is located at time 700 s and 1150 s.

Further exposure of the same sensor to hydrogen sulfide no longer lead to additional phase shift (time 1150) since all lead ions have already reacted with a sulfur atom and the sensing layer is saturated. This integrative measurement is considered as a feature of the sensor since measurement campaigns separated in time will still allow for detecting pollution plumes even if the GPR is not collecting sensor echoes at the time the gas reaches the sensing surface. It is assumed that such sensors are relevant in scenarios in which the consequence of the pollution overwhelms the loss of the sensor whose sensing layer has been saturated, and a new batch of sensors is inserted in new boreholes once the cause of the pollution has been identified and cared for.

The sensor saturated response reaches several tens of phase degrees rotation, well above the baseline phase standard deviation of the wireless GPR measurement of the sensor characteristics, confirming that the Sensors & Software pulseEkko GPR controlled by the SPIDAR unit is well suited for such an application. This analysis hints at a detection limit of 1% of the saturated response since the 120° phase shift of the 200 MHz (5 ns-period) delay response accounts for $5/3 = 1.66$ ns or 1% of the 11 ps jitter observed when qualifying the SPIDAR control unit.

VI. Embedded network analyzer alternative

While GPR are basic instruments, they are hardly affordable for on site long term measurements. Furthermore, Vector Network Analyzer (VNA) have been demonstrated to exhibit improved stability with respect to pulsed mode GPR [10]. The proliferation of embedded radiofrequency frontends such as Analog Devices AD976x or Silicon Labs Si5321 has led to multiple implementations of embedded network analyzers, including the opensource/openhardware NanoVNA as described at https://nanovna.com/. The frequency band – from 50 to 900 MHz – is ideally suited to probing sub-GHz

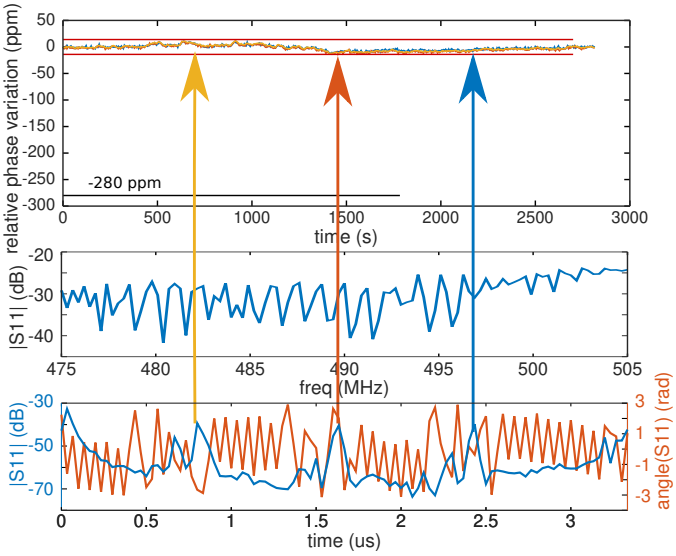

Fig. 9. Relative phase variations of three echoes with delays of 0.8 (yellow arrow), 1.6 (orange arrow) and 2.4 μs (blue arrow) as probed by a NanoVNA embedded network analyzer on a 30 MHz bandwidth and extracted from the inverse Fourier transform. The raw phase variation curves (top) are framed with two horizontal red lines matching the phase variation expected from ± 0.2 K temperature variation – representative of temperature fluctuations over the measurement time scale assuming a 70 ppm/K temperature sensitivity – while the black horizontal line at position -280 ppm matches the phase variation expected from gas absorption in the sensing layer. Middle is one frequency domain and bottom is one time-domain transfer function with the arrows indicating the position at which the phases were measured when computing the top phase-evolution chart.

SAW cooperative targets, and number of sampled frequencies limited to 101 is hardly an obstacle to the short response delay of these transducers. Indeed with a 30 MHz bandwidth at 490 MHz limited by piezoelectric electromechanical coupling of lithium niobate YXl/128° (5% or 24.5 MHz bandwidth), the time resolution of the inverse Fourier transform of the frequency swept reflection coefficient characteristics is 33 ns or a total duration of 3.33 μs. From an engineering perspective, clocking a frequency swept synthesis from a stable reference is readily achieved by selecting a temperature compensated or over controlled quartz crystal oscillator, while providing a stable high bandwidth sampling system as used in the pulsed mode RADAR shown above appears more challenging.

Fig. 9 exhibits the phase stability of three echoes of a 490 MHz reflective delay line sampled in a wired configuration every 5.33 s by a NanoVNA. The red lines at ± 14 ppm indicate the ± 0.2 K room temperature variation observed during the acquisition, while the -280 ppm black line (selected as one tenth of the phase variation observed in Fig. 8) indicates the expected phase variation induced by chemical sensing layer mass loading, well above the noise limit of the instrument. Hence, such Voltage Controlled Temperature Compensated Crystal Oscillator (VCTCXO) are credible alternatives for long term, embedded on site measurement of sub-surface sensors (Fig. 9).

VII. Conclusion

We demonstrate sub-surface pollutant detection using a Sensors & Software pulseEkko GPR operating at either 100 or 200 MHz. Dedicated reflective surface acoustic wave delay lines have been designed and functionalized to operate as cooperative targets. Echoes returned by the delay lines are recorded by the GPR, with time delay between echoes representative of the acoustic velocity, here varying upon exposure to hydrogen sulfide thanks to the functionalization with a thin polymer film including lead ions reactive to sulfur.

During this investigation initially focusing on long term stability assessment of the GPR sampling rate, we have identified a short term fluctuation of the sampling rate with a period of 200 ns and a range of ± 1.5 ns. Finally, an embedded vector network analyzer exhibits the targeted stability thanks to the high quality reference oscillator, demonstrating how a frequency sweep approach followed by an inverse Fourier to recover the time-domain response provides an alternative to the pulsed mode stroboscopic GPR architecture. Further investigations will assess the impact of replacing the VCTCXO with an oven-controlled crystal oscillator in order to improve the long term baseline stability of the embedded vector network analyzer solution.

Acknowledgements

This work was completed in the framework of the UNDERGROUND grant from the French National Research Agency (ANR-17-CE24-0037). The radiofrequency-grade oscilloscope was acquired thanks to the Oscillator IMP grant. SAW devices were manufactured in the MIMENTO cleanroom facility of FEMTO-ST (Besançon, France) supported by the RENATECH network.

References

[1] C. Campbell, *Surface Acoustic Wave Devices for Mobile and Wireless Communications*. Academic press, 1998.

[2] D. Morgan, *Surface acoustic wave filters: With applications to electronic communications and signal processing*. Academic Press, 2010.

[3] K.-Y. Hashimoto, *Surface acoustic wave devices in telecommunications*. Springer, 2000.

[4] J.-M. Friedt, T. Retornaz, S. Alzuaga, T. Baron, G. Martin, T. Laroche, S. Ballandras, M. Griselin, and J.-P. Simonnet, "Surface acoustic wave devices as passive buried sensors," *Journal of Applied Physics*, vol. 109, no. 3, p. 034905, 2011.

[5] S. Talmaki, S. Dong, and V. R. Kamat, "Comprehensive collision avoidance system for buried utilities," in *Proceedings of the 2010 International Conference on Sustainable Urbanization (ICSU), Hong Kong Polytechnic University, Hong Kong*, 2010, pp. 1265–1274.

[6] D. Wu and X. Zhang, "Assessing governance issues of underground utility as-built records," in *Geo-Informatics in Resource Management and Sustainable Ecosystem*. Springer, 2015, pp. 3–8.

[7] D. Johannsmann, *The quartz crystal microbalance in soft matter research – Fundamentals and modeling*. Springer International Publishing (Switzerland), 2015.

[8] M. Paquit, L. Arapan, W. Feng, and J.-M. Friedt, "Long range passive RADAR interrogation of subsurface acoustic passive wireless sensors using terrestrial television signals," *IEEE Sensors Journal*, 2020.

[9] J.-M. Friedt, "Passive cooperative targets for subsurface physical and chemical measurements: a systems perspective," *IEEE Geoscience and Remote Sensing Letters*, vol. 14, no. 6, pp. 821–825, 2017.

[10] H. Liu, B. Xing, J. Zhu, B. Zhou, F. Wang, X. Xie, and Q. H. Liu, "Quantitative stability analysis of ground penetrating radar systems," *IEEE Geoscience and Remote Sensing Letters*, vol. 15, no. 4, pp. 522–526, 2018.

[11] M. T. Taner, F. Koehler, and R. Sheriff, "Complex seismic trace analysis," *Geophysics*, vol. 44, no. 6, pp. 1041–1063, 1979.

[12] D. Rabus, F. Minary, G. Martin, and J.-M. Friedt, "A high-stability dual-chip GPR for cooperative target probing," in *2018 17th International Conference on Ground Penetrating Radar (GPR)*. IEEE, 2018, pp. 1–4.

[13] D. Rabus, J.-M. Friedt, L. Arapan, S. Lamare, M. Baqué, G. Audouin, and F. Chérioux, "Sub-surface H_2S detection by a surface acoustic wave passive wireless sensor interrogated with a ground penetrating radar," *ACS Sensors*, 2020.